

# Chapter 6

## Poly Methyl Methacrylate (Pmma) Based Polyaniline Composite for Ammonia (Nh3) Gas Sensors

Muktikanta Panigrahi <sup>1,\*</sup>, Basudam Adhikari <sup>1</sup>

<sup>1</sup> Materials Science Centre, Indian Institute of Technology, Kharagpur, West Bengal, India

\*Corresponding author: [muktikanta2@gmail.com](mailto:muktikanta2@gmail.com)

### Abstract

Inorganic acids (HCl, H<sub>2</sub>SO<sub>4</sub>, and H<sub>3</sub>PO<sub>4</sub>) doped-PMMA/PANI composites are prepared by *in-situ* technique via oxidation-polymerization process. Different techniques such as XRD, FTIR, UV-Visible, four-probe method are used to characterize the composite. Presence of different chemical group of the doped composites is analysed by ATR-FTIR spectroscopic analysis. Charge carrier behaviour of the doped composite is analyzed by UV-Visible spectroscopy. Band gap ( $E_g$ ) of the doped composites is determined from UV-Visible absorption analysis using Tauc expression. The estimated direct band gap energy ( $E_g$ ) is found to be 1.93 eV (for HCl doped PMMA/PANI composite), 1.19 eV (for H<sub>2</sub>SO<sub>4</sub> doped PMMA/PANI composite), and 1.71 eV (for H<sub>3</sub>PO<sub>4</sub> doped PMMA/PANI composite), respectively. DC-conductivity is measured with and without magnetic field. Temperature dependent DC conductivity is also measured. In addition, we were discussed the response of ammonia (NH<sub>3</sub>) gas with polyaniline-based sensor materials.

**Key Words:** PMMA, PANI-ES, Dopant, UV-Visible, Band Gap, Conductivity (with and without) magnetic field, Organic Semiconductor

### Introduction

Conducting polymers with extended  $\pi$ -electrons conjugation are highly susceptible to chemical or electrochemical oxidation or reduction. Conducting polymers have established to have suitable properties for technological applications such as electroluminescent device [1], field effect transistor [2], chemical sensor [3], electrode [4], metal anticorrosion [5], marine fouling prevention [6].

© IOR INTERNATIONAL PRESS, 2021

Muktikanta Panigrahi & Basudam Adhikari 1, *Poly Methyl Methacrylate (Pmma) Based Polyaniline Composite for Ammonia (Nh3) Gas Sensors*,

<https://doi.org/10.34256/ioriip2126>

In the conducting polymer family, polyaniline (PANI) occupies an important position in the family, which is inherently present conductivity. The conducting polymer is called intrinsic conducting polymer (ICP). PANI is synthesized by different routes such as chemical and electrochemical method. It has low cost of synthesis with good environmental stability and unique acid-base doping-dedoping [7-9]. In spite of its several desirable properties, there is some limitations *viz.* insolubility in conventional solvents for processing [10] and poor mechanical strength [4,5]. One of the ways to overcome these demerits that is to prepare conducting composites using an insulating polymer matrix [11]. Researchers have devoted to prepare polyaniline composite with insulating polymers. The composite show enhanced structural and electronic stability in different atmospheres. Several popularly used matrix polymers employed are poly (vinyl acetate) [12], poly (vinyl chloride) [13], poly(methyl methacrylate) [14], polystyrene [15], poly urethane [16], polylactide [17], and poly(vinyl pyrrolidone) (PVP) [18]. PVP surface can adsorb the electroactive polymer, forming a solvated steric barrier around individual particles, thus preventing aggregation and increasing dispersion [18]. If PANI is encapsulated, PVP can enhance the electrical conductivity of polyaniline by trapping gases inside its matrix, thus allowing increased gas surface interactions between the analytes and PANI particles. Guixin et al. [19] prepared electrically conductive biodegradable composite from polypyrrole and poly (D,L-lactide) by emulsion polymerization followed by precipitation. Huang and his co-workers [20] synthesized a block copolymer having polylactide covalently bonded to an electroactive polymer, such as PANI which could exhibit improved solubility, and processibility of electroactive materials.

To investigate the optical properties of conducting polymer composite have attracted great attention because of their technological applications such as optical sensors [21], antireflective coatings [22]. Both optical band gap and refractive index are the key parameter of an optical material. Since, these are closely related to the electronic properties of materials.

In the current work, author is reported synthesis of doped PMMA/PANI composites using liq. aniline as precursor *via in situ* polymerization route. HCl, H<sub>2</sub>SO<sub>4</sub>, and H<sub>3</sub>PO<sub>4</sub> are used as dopants, which is inorganic in nature. We analyzed the effect of dopants *i.e.*, HCl, H<sub>2</sub>SO<sub>4</sub>, H<sub>3</sub>PO<sub>4</sub> on crystallinity, charge transfer spectra, band gap and room temperature DC conductivity with and without magnetic field in doped PMMA/PANI composite(s). Also, estimated temperature variation DC conductivity.

## **Experimental Details**

### **Chemicals and Materials**

Reagent grade chemicals such as aniline liquid, ammonium persulfate, hydrochloric acid, sulphuric acid, ortho-phosphoric acid, diethyl ether are procured from Merck, India. Poly (methylmethacrylate) (PMMA) is used as base materials, which is purchased from local market as sheet. This is used during the preparation of

PMMA/PANI composite.

### **Pmma/Pani Composite Preparation (*In-Situ*)**

Both polymer (*i.e.*, PMMA polymer piece, small) and chloroform (*i.e.*, CHCl<sub>3</sub>) are taken in a 100 mL beaker. The mixture is stirred (upto 3 h) to form a transparent mass solution. The mass solution is poured and cast into a flat petridis (diameter= 5 inches). The film (*i.e.*, cast mass) is removed from petridis after solvent evaporation. The film is cut into small pieces (1.5 ×1.5 cm) and is used during the preparation of composite.

PMMA/PANI composite is prepared by chemical-oxidation method using liquid aniline (conducting polymeric material) and PMMA film (base materials). The composite preparation is carried out at room temperature [23]. The composite is prepared in **three steps**. In **step one**; dopant solution is prepared by taking distilled water and concentrated HCl in appropriate proportion. In **step two**, oxidant solution is taken into account. 7.47 g of ammonium persulphate (APS) is added slowly to 60 mL of 1(M) HCl solution with shaking (5 minutes). 3 mL of liquid aniline and PMMA films (1.5 cm × 1.5 cm) are put into the 500 mL conical flask contained 105 mL of 1 (M) HCl solution. It is stirred (with 600 rpm) up to 12 h in a magnetic stirrer. To this solution, APS solution is added drop wise with continuous stirring. The polymerization is carried out and is mentioned in **third step**. The reaction mixture is stirred for 10 h. The color of transparent PMMA films became light green to dark green. The composites are washed with distilled water several times followed by dry up in air for 6 h. For comparison, H<sub>2</sub>SO<sub>4</sub>, doped PMMA/PANI composite and H<sub>3</sub>PO<sub>4</sub> doped PMMA/PANI composites are also prepared under same conditions.

### **Characterization Techniques**

X-ray diffraction experiments PMMA film, PANI, and doped PMMA/PANI composite are executed using a Phillips PW-1710 advance wide angle X-ray diffractometer, Phillips PW-1729 X-ray generator, CuK $\alpha$  radiation,  $\lambda = 0.154$  nm. The generator is operated at 40 kV and 20 mA. The film/powder samples are tested. Samples are placed on a quartz sample holder at room temperature. The scanned diffraction angle is 10° to 50° (2 $\theta$ ) with scanning rate (2°/min).

ATR-FTIR spectra are recorded on a Thermo Nicolet Nexus 870 spectrophotometer (from 400 to 4000 cm<sup>-1</sup>). ATR-FTIR spectrometer settings are kept constant (50 scan at 4cm<sup>-1</sup> resolution, Absorbance measurement mode). Film/powder samples are tested. For powder samples particularly PANI, pallet is prepared using potassium Bromide (KBr) through compression molding with pelletizer. Before running the samples, a background spectrum is collected. Then samples are put in a sample holder and data are collected.

Doped PMMA/PANI composite is used during UV-Visible analysis. The spectra of the composites are recorded by using a Micropack UV-VIS-NIR, DH 2000.

The wave length region of the analysis is 250-1000 nm. Base line is corrected before recording the spectra. Optical band gaps are determined from UV-Visible analysis.

Raman spectra are noted on a Renishaw Raman imaging microscope (System 3000) containing a Olympus metallurgical microscope and a CCD detector (cooled by a Peltier) using 632.8 nm exciting radiation (He-Ne laser, Spectra Physics, model 127). 457.9, 488.0, and 514.5 nm exciting radiations (Ar<sup>+</sup> laser, Omnichrome model 543-AP) are done. The laser beam is focused on the sample in a roughly 1  $\mu$ m spot by a  $\times$  80 lens. The laser power is always kept below 0.7 mW for avoiding sample degradation. FT-Raman spectra of the samples are recorded in an RFS 100 FT-Raman Bruker spectrometer with the 1064 nm radiation (Nd:YAG laser). Solid samples are taken for Raman study.

Surface morphology of PMMA polymer film, PANI, and PMMA/PANI composite are analyzed by scanning electron microscopy (Carl Zeiss Supra 40). Samples are coated with gold before the measurement.

DC-conductivity of the doped composite (with and without magnetic field) at room temperature is measured using a linear four-probe technique. DC-conductivity are calculated using the relation  $\rho=2\pi S (V/I)$  where S is the probe spacing (mm), 'I' is the supplied current (nA) and 'V' is the corresponding voltage (mV). The conductivity ( $\sigma$ ) is calculated using the expression  $\sigma=1/ \rho$  [23].

Magneto-resistivity is investigated using a Helium Compressor (HC) (model HC-4E1) –sumitomo cryostat (model Ganis research CO, INC) equipped with 0.8T superconducting magnet (Lake shore electromagnet). Lake Shore 331 temperature controller is used. The measurement(s) are performed in the temperature range 77-300 K using a computer-controller measuring system.

## Results and Discussion

XRD patterns for HCl doped PMMA/PANI composite, H<sub>2</sub>SO<sub>4</sub> doped PMMA/PANI composite, and H<sub>3</sub>PO<sub>4</sub> doped PMMA/PANI composite are shown in **Figure 1**. The PMMA film show a highly broaden peak, indicating their amorphous nature [24]. But, doped PMMA/PANI composites show certain peaks which is due to crystalline structure exhibit well defined crystalline peaks at  $2\theta$  of 22.4°, 30°, and 42°, respectively. It is also observed that the peak area is reduced and is slightly shifted to higher angle in the composites. Therefore, This may be happened due to the combined effect of polyaniline and presence of dopant (HCl or H<sub>2</sub>SO<sub>4</sub> or H<sub>3</sub>PO<sub>4</sub>) with retaining PMMA structure [25].

The typical absorption peaks of PMMA film, PANI-ES and doped PMMA/PANI composites are shown in **Figure 2**. The bands of PMMA film are observed at 2965, 1751, 1626, 1221  $\text{cm}^{-1}$  in the **Figure 2** [25]. It is attributed to C-H stretching, C=O stretching, C-O stretching of ester, and C-O-C stretching vibration respectively. The bands at 1448, 1364, 1358  $\text{cm}^{-1}$  represent the stretching vibration of C-H deformation of PMMA film. The peaks at 1253, 1184, 1134, 1047  $\text{cm}^{-1}$

correspond to aliphatic  $-C-H$  in plane bending of PMMA [25]. These indicate that the characteristic absorption features of PMMA film are retained in the prepared PMMA films. FTIR bands of PANI are found at  $1554, 1475, 1108\text{ cm}^{-1}$ . This is corresponded to quinoid, benzenoid, and  $C=N$  stretching respectively [25].

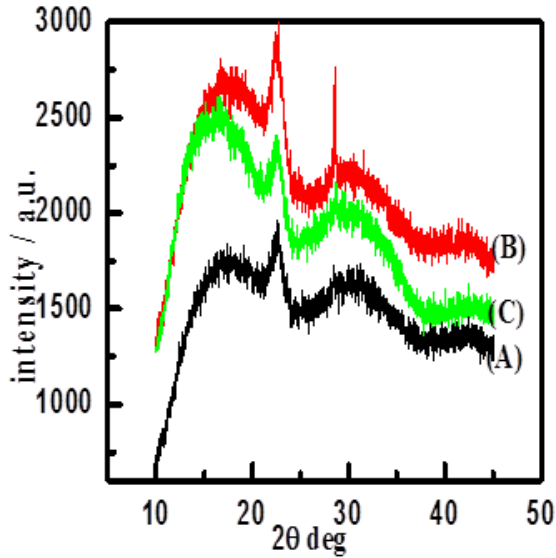


**Figure 1.** XRD pattern of HCl (A),  $H_2SO_4$  (B), and  $H_3PO_4$  (C) doped PMMA/PANI composites

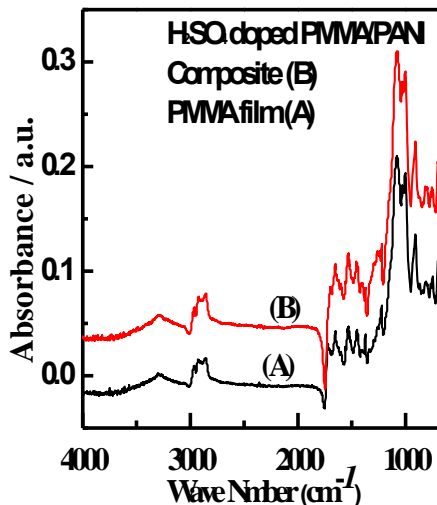


**Figure 2.** ATR-FTIR spectra of PMMA film (A) and  $H_2SO_4$  doped PMMA/PANI-ES composites (B)

From our remark, spectrum of H<sub>2</sub>SO<sub>4</sub> doped PMMA/PANI composites are exhibited the presence of quinoid and benzenoid ring vibrations at 1475, and 1554 cm<sup>-1</sup> respectively. This is indicated the occurrence of oxidation state of PANI [24]. This indicates the formation of conducting PMMA film.

In the literature, PANI shows different electronic transitions such as  $\pi$ - $\pi^*$  of benzene ring, polaron to  $\pi^*$ , benzenoid to quinoid ring and polaron transition, respectively [26, 27]. No polaron transition is found in spectrum of PMMA film [24]. H<sub>2</sub>SO<sub>4</sub> doped PMMA/PANI composite is conducted optical studies with the use of a UV-visible (UV-VIS) spectroscopic technique and is shown in **Figure 3**. Results show that the absorption of photon energy by organic molecules in the UV-VIS region caused an upward transition of electrons in the n,  $\sigma$ , and  $\pi$  orbitals. Various electronic transitions correspond to the different bands present in the samples. In **Fig. 3**, bands like  $\pi$  to localized polaron band of H<sub>2</sub>SO<sub>4</sub> doped PMMA/PANI composite is observed. Polaron band is suggested to the presence of oxidation unit *i.e.*, formed emeraldine salt [26, 27]. Hence, electrons are delocalized in the excitation band [26, 27]

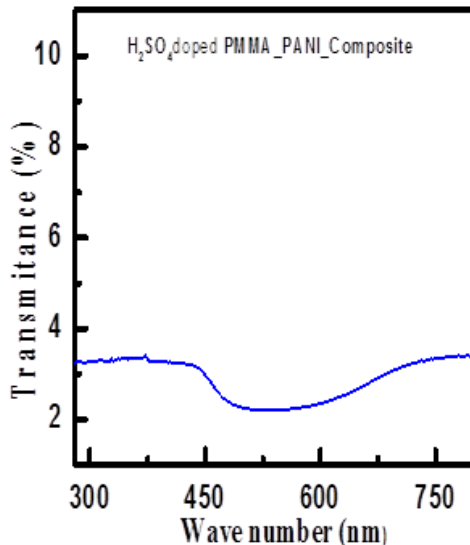


**Figure 3.** UV-Vis spectrum of H<sub>2</sub>SO<sub>4</sub> doped PMMA/PANI composites

The photon absorption of organic semiconductor is observed by Tauc expression [28, 29].

$$(\infty hv) = A (hv - E_g)^n \dots\dots\dots (1)$$

Where  $\infty$  = optical absorption co-efficient,  $h\nu$  = photon energy,  $E_g$  = Energy gap calculated from graph,  $A$  = absorption constant,  $n$  = represents the type of transition occurs. If  $m = 2$  indicated allowed indirect transitions and  $m = 1/2$  indicated allowed direct transitions [28, 29].

$$A = \alpha bc = -\ln T \dots\dots\dots (2)$$

$$\alpha = -\ln T / bc \dots\dots\dots (3)$$

Substituting ‘ $\alpha$ ’ in equation (1),

Then,  $[(-\ln T / bc) hv] = A (hv - E_g)^m$

$[(-\ln T) (hv)] = B(hv - E_g)^m$

Where;

b= thickness of samples

c=concentration of samples

T=transmittance

B=another constant.

**Table 1** Direct and indirect band gap of doped PMMA/PANI Composites

<b>Prepared materials name</b>	<b>Direct allowed band gap (eV)</b>	<b>Indirect allowed band gap (eV)</b>
H <sub>2</sub> SO <sub>4</sub> doped PMMA_PANI_Composite	<b>1.19</b>	<b>0.17</b>
H <sub>3</sub> PO <sub>4</sub> doped PMMA_PANI_Composite	<b>1.71</b>	<b>0.65</b>
HCl doped PMMA_PANI_Composite	<b>1.93</b>	<b>0.853</b>

For direct transition can plot  $(\alpha hv)^2$  vs hv, and extrapolate the linear portion of it to  $\alpha=0$  value to obtained corresponding direct band gap. Similarly, the intercept of these curves on the photon energy axis (hv) gives the indirect band gap [28, 29]. The direct and indirect allowed transitions energies of three prepared composites are listed in **Table xxx**. To estimated direct band gap of doped PMMA/PANI (1M H<sub>2</sub>SO<sub>4</sub>), doped PMMA/PANI (1M H<sub>3</sub>PO<sub>4</sub>) and doped PMMA/PANI (1M HCl) are found to be 1.19 eV, 1.71 eV, and 1.93 eV respectively. The variations of band gap values are due to the incorporation of used dopants into the polymer chain. The dopants strength is in the order of HCl < H<sub>3</sub>PO<sub>4</sub> < H<sub>2</sub>SO<sub>4</sub>. The lower strength dopant exerts less force against ordering and closing of the polymer chains leading to a lower density of states into the visible region [28, 29].

The morphologies of PMMA film and PMMA/PANI composite are evaluated with Raman spectrophotometer and is shown Figure 4. Figure 4A *i.e.*, morphologies of PMMA film shows different sizes speherical domains. Magnification of the image is 10X. The morphology of H<sub>2</sub>SO<sub>4</sub> doped PMMA/PANI composite is indicated in Figure 4B with 10X magnification. H<sub>2</sub>SO<sub>4</sub> doped PMMA/PANI composite is getting solid fibers or rods. This is happened due to reaction of H<sub>2</sub>SO<sub>4</sub>

dopants and polyaniline salt with PMMA films.

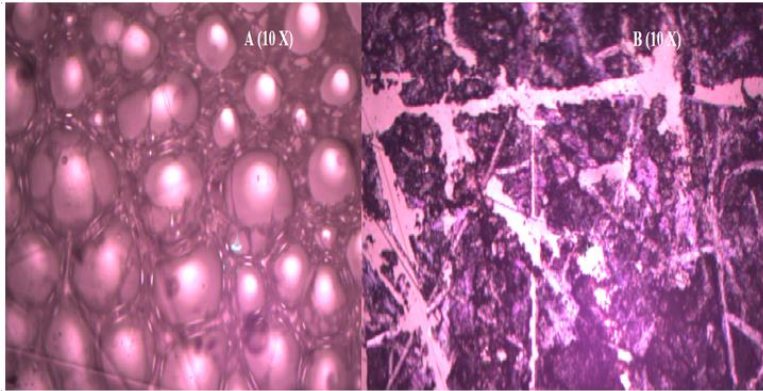


**Figure 4.** Image of PMMA flim (A) and H2SO4 doped PMMA/PANI Composite (B)

SEM images for pure PMMA polymer film and doped PMMA/PANI Composites are shown in Figure 1.

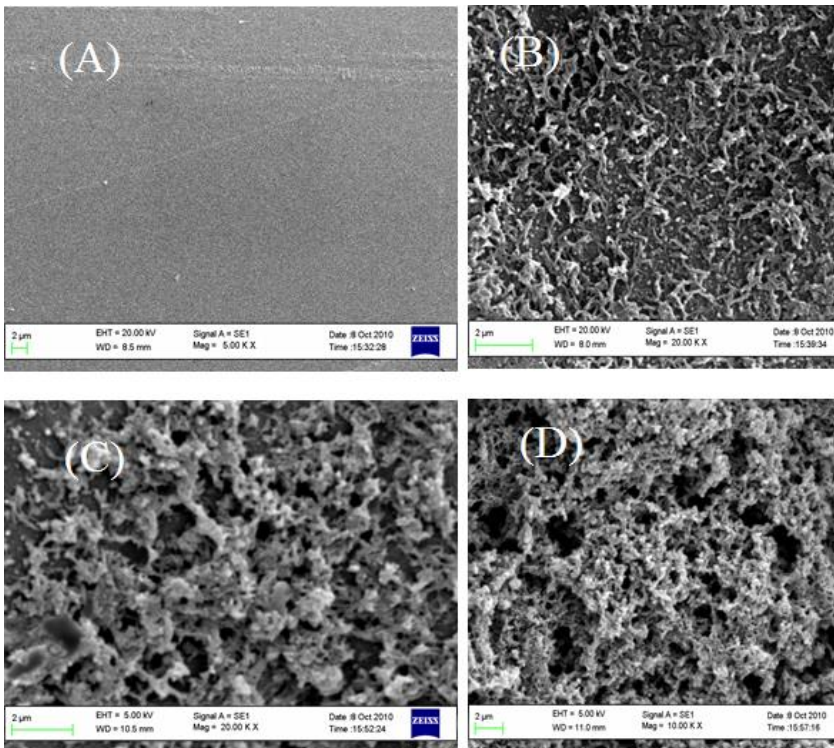
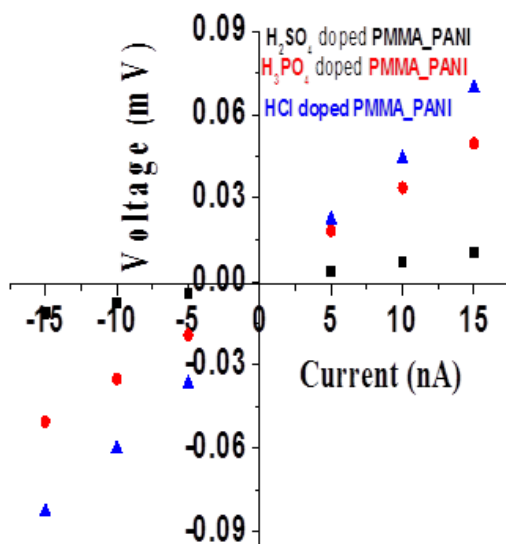


**Figure 1** FESEM images of PMMA polymer film (A), 1 M HCl doped

PMMA PANI composite (B), 1 M H<sub>3</sub>PO<sub>4</sub> doped PMMA PANI composite (C), and 1 M H<sub>2</sub>SO<sub>4</sub> doped PMMA PANI composite (D)

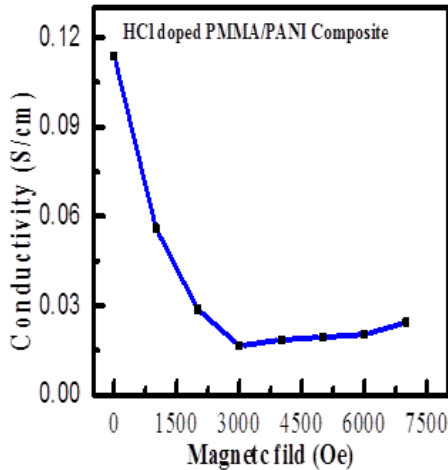
Smooth texture is observed in Fig.1A, whereas fibrous structures are showed in all doped PMMA/PANI Composites. Three dopants viz., HCl, H<sub>2</sub>SO<sub>4</sub> and H<sub>3</sub>PO<sub>4</sub> are used to prepare doped PMMA/PANI Composites. It is also found that size and formation probability of PANI is strongly dependent on dopant strength, structure and reaction conditions. Moreover, the diameter size of PANI nano-fibrous is affected by dopant structure. Average (av.) diameters of PMMA/PANI composites are found to be 178 nm, 152 nm, and 165 nm, respectively. The diameter is related to aspect ratio *i.e.*, surface area/volume. The surface area of nanofibers increases as the average diameter of nanofibers decreases. it could be important, particularly for gas sensor application.

The plot of room temperature DC-conductivity of HCl-, H<sub>2</sub>SO<sub>4</sub>- and H<sub>3</sub>PO<sub>4</sub>-doped PMMA/PANI composites are shown in **Figure 5**. It is observed from the **Figure 5**; the voltage (mV) is linearly related with current (nA) and passes through origin, indicating that the ohmic behaviour. The conductivity of prepared conductive composite is presented in Table 1, it is clear from the Table, the conductivity of H<sub>2</sub>SO<sub>4</sub>-doped PMMA/PANI composite showed  $0.1497 \times 10^{-2}$  S/cm at 0 Tesla which is higher than other two as-prepared doped PMMA/PANI composite at 0 tesla. This is due to higher strength dopant. The higher strength dopants exert less force against ordering and closing of polymer chains leading to higher compactness of polymer chains. The compactness is a favorable factor for intramolecular mobility of charged species along the chain and some extent inter molecular hopping because of better and closer packing and hence, higher conductivity than the later one [8]. Also, The DC conductivity is observed for H<sub>2</sub>SO<sub>4</sub>-doped PMMA/PANI composite ( $0.1421 \times 10^{-2}$  S/cm) at 0.4 tesla.



**Figurer 5** DC conductivity of HCl (A), H2SO4 (B), and H3PO4 (C) doped PMMA/PANI composites measured at room temperature without magnetic field

The plot of room temperature DC-conductivity with magnetic field (from 0 Oe to 7500 Oe) of HCl-doped PMMA/PANI composites is shown in **Figure 6**. It is observed from the **Figure 6** that the DC conductivity decreases with increase in magnetic field. This is due to electron-scattering mechanisms of the composite [31].



**Figurer 6.** DC conductivity of HCl doped PMMA/PANI composites measured at room temperature with magnetic field

**Figure 7** indicates temperature variation DC conductivity of HCl doped PMMA/PANI composite. It is evident from the **Figure 7**, DC conductivity of composite increases with increase in temperature.

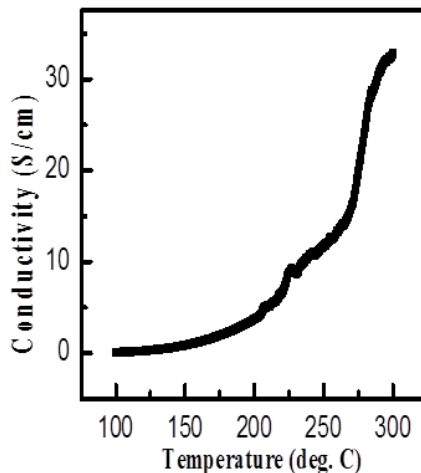


**Figure 7.** Temperature dependent DC conductivity of HCl doped PMMA/PANI composites measured at 0 Oe magnetic field

It means that prepared conductive composite represent a temperature dependent conductivity, which is similar behaviour to an inorganic semiconductor. Henceforth, it is termed as organic semiconductor [8].

### Response of Ammonia (Nh3) Gas

Monitoring of ammonia gases is a vital issue in the environment due to their high toxic nature of the gas. The toxicity limit of ammonia for human exposure is found to be 25 ppm for 8 h [31]. Traditional method for detecting ammonia gas by chemical analysis is a time-consuming and complicated process. This method is not suitable for analyzing the NH<sub>3</sub> gas. Hence, there is an increasing mandate for a sensor, which has fast, non-destructive and reliable. Metal oxide based sensors such as SnO<sub>2</sub> or Fe<sub>2</sub>O<sub>3</sub> are sensitive to detect low levels of concentration. The operation of sensors requires high temperatures, which increases cost and complexity of these devices [32]. Researchers put their effort to discover monitoring system, which is operated at ambient temperature. The new type of sensor materials are conducting polymer based materials and it is operated at room temperature [33] at lower concentration level.

Conducting polymers are a new class of sensors material due to their diversity, ease of synthesis, doping/de-doping behaviour and sensitivity at ambient temperature [34-36]. The gas sensor performance of a conducting polymer based sensor materials is depended on electrical or optical properties. The changes of electrical properties are directly related to the adsorption of analytes concentration at ppm levels on sensor materials surface [37, 38]. Some reports on specificity and sensitivity of conducting polymer based sensors are available even at low concentration (ppm) of analytes gases. It is achieved either by incorporating functional groups or doping to the main chain of conducting polymer [39, 40]. A few works are reported on the ammonia gas sensing of polyaniline, polypyrrole, Polythiophene and their composites [41-43]. Conducting polymer films devices have been used to sense ammonia gas in the range of 10–5000 ppm concentration. Sensor characteristics such as fast response, rapid recovery and detection at low concentration level i.e., ppm level are still key concerns to commercialize the conducting polymer-based sensor. Conducting polymer thin films based sensor materials are projected to give better response and recovery than conducting polymer based sensor. The schematic diagram of possible ammonia sensing mechanism is shown in Figure 8.

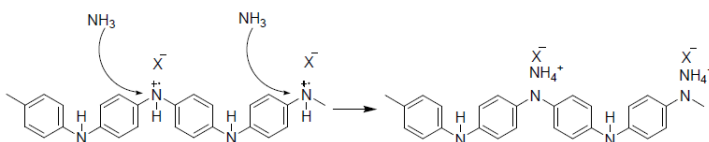


**Figure 8.** Possible polyaniline with ammonia sensor mechanism [44]

Particularly, polyaniline is one of the conducting polymer families. It is controlled by acid/base reactions in doped state. Therefore, polyaniline is extensively used to detect acidic and basic gases. When exposed ammonia gas on polyaniline, it undergoes dedoping by deprotonation [45-50]. The protons on –NH– groups of polyaniline backbone are transferred to NH<sub>3</sub> molecules and formed ammonium ions. Polyaniline itself formed base. The process is reversible. When ammonia atmosphere is removed, the ammonium ion can be decomposed to ammonia gas and proton.

The extent of response and rapid recovery is dependent on the methods used to prepare thin film. Ultra-thin films of conducting polymers have very high aspect ratio. It can allow the gas molecules on the film surface to produce large and rapid change of the chemical or physical properties, which is leading to enhance sensitivity of the device [51].

**Table 2.** Brief summary of CO detection

Study	Materials	Perporfance	Optimum temperature	Limitation
Yadav et al. [54]	PANI-DBSA	Response time 329 s	Room temperature	Contact potential suddenly increased
Lv et al.[55]	PSS-PANI/PVDF composite	Response 70%	Room temperature	Low NH <sub>3</sub> concentration
Sutar et al. [56]	Polyaniline nanofiber	Response time 1-5 s	Room temperature	Low NH <sub>3</sub> concentration
Crowley et al.[57]	polyaniline nanoparticles	Response 15 s	Room temperature	Humidity dependency Humidity dependency and
Matsuguchi et al. [58]	PANI-PMMA blend film	RH 68%	Room temperature	conductivity decreases on exposing ammonia gas
Matsuguchi et al.[59]	PANI-PMMA blend film		Room temperature	High concentration of NH <sub>3</sub> gas (600 ppm)
Deshpande et al.[60]	Polyaniline SnO <sub>2</sub> nanocomposite	Response 37%	Room temperature	High concentration of NH <sub>3</sub> gas (500 ppm)

Tai et al.[61]	PANI/TiO <sub>2</sub> thin film	Room temperature	High concentration of NH <sub>3</sub> gas (2500 ppm)
----------------	---------------------------------	------------------	--

In this perspective, one of the thin film technologies is Langmuir–Blodgett technique. It can be used to produce very regular multilayers, and well-defined molecular orientation [52, 53]. The sensor materials fabricated using this technique is expected to have higher sensitivity, faster response time and good reproducibility. The brief summary carbon monoxide detection is presented in Table 2.

**Fig. 9** shows the relative response of a typical material as a function of NH<sub>3</sub> concentration. Relative response is estimated using  $(R-R_0)/R_0$ , where  $R_0$  is the initial resistance in the absence of NH<sub>3</sub> and  $R$  is the saturation value of resistance measured on exposure to gas. It is saturate at higher concentrations. This is due to the availability of a limited number of reactive species in the layer of sensing materials. The fast response is accredited to high aspect ratio, which is offered by nanofibrous morphology. Hence, nanostructures help to easy diffusion of NH<sub>3</sub> gas. The different ammonia concentration exposure vs time of polyaniline based martials is shown in Figure 9.

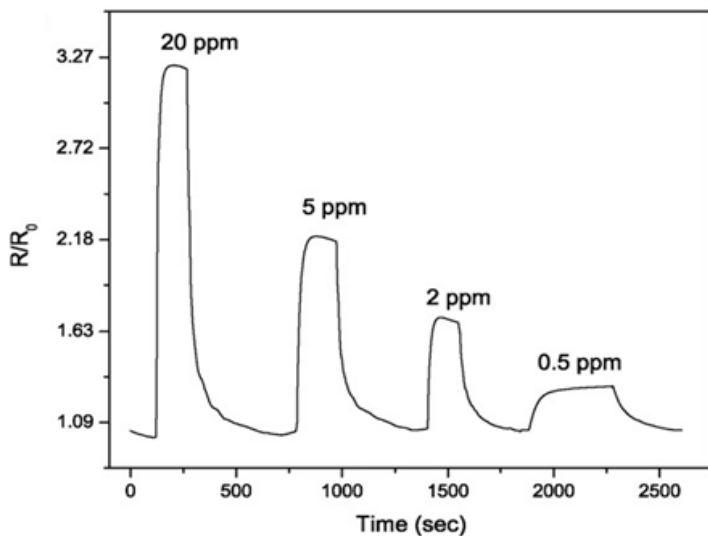


**Figure 9.** Plot of different ammonia concentration exposure vs time of polyaniline based martials [56]

## Conclusions

PMMA/PANI composite films are prepared by *insitu* polymerization technique. HCl, H<sub>2</sub>SO<sub>4</sub>, and H<sub>3</sub>PO<sub>4</sub> are used dopants, separately, during the

polymerization reaction. Different desired chemical groups of PMMA film, PANI and PMMA/PANI composites are confirmed from ATR-FTIR spectroscopy. Polaron band is shown in UV-Visible data and are confirmed the formation of emeraldine salt (ES). A drastic increment of band gap of the doped samples is found. I-V characteristics without magnetic field of doped PMMA/PANI composites are revealed ohmic behaviour at room temperature. Highest DC conductivity without magnetic field is found to be  $0.1421 \times 10^{-2}$  S/cm for H<sub>2</sub>SO<sub>4</sub> doped PMMA/PANI composite. Decreased DC conductivity data with increased magnetic field is observed. Temperature dependent DC conductivity data of HCl doped composite is indicated the semiconducting behaviour. In particulars, ammonia gas responses and mechanism of polyaniline-based materials are discussed.

## Acknowledgments

The author conveys their sincere thanks to the CRF, IIT Kharagpur for their providing testing facilities and Materials Science Centre to do the research work.

## References

- [1] Burroughes, J.H., Bradley, D.D.C., Brown, A.R., Marks, R.N., Mackay, K., Friend, R.H., Burns, P.L., and Holmes, A.B. 1990, Light-emitting Diodes Based on Conjugated Polymers, *Nature*, Vol. 347, pp. 539-541.
- [2] Frackowiak, E., Khomenko, V., Jurewicz, K., Lota, K., and Beguin, F. 2006, Supercapacitors Based on Conducting Polymers/Nanotubes Composites, *Journal of Power Sources*, Vol. 153, pp. 413-418.
- [3] Conn, C., Sestak, S., Baker, A.T., and Unsworth, J. 1998, A Polyaniline-Based Selective Hydrogen Sensor, *Electroanalysis*, Vol. 10, pp. 1137-1141.
- [4] Abdelkader, R., Amine, H., and Mohammed, B. 2012, Thermally Stable Forms of Pure Polyaniline Catalyzed by Acid-exchanged Montmorillonite Clay called Maghnite-H<sup>+</sup> as an Effective Catalyst, *International Journal of polymer science*, Vol. 2012, pp. 1-7.
- [5] Yang, S. and Ruckenstein, E. 1993, Processable Conductive Composites of Polyaniline/Poly (alkyl methacrylate) Prepared via an Emulsion Method, *Synthetic Metals*, Vol. 59, pp. 1-12.
- [6] Singh, V., Mohan, S., Singh, G., Pandey, P.C., and Prakash, R, 2008, Synthesis and Characterization of Polyaniline-carboxylated PVC Composites: Application in Development of Ammonia Sensor, *Sensors and Actuators B: Chemical* Vol. 132, pp. 99-106.
- [7] Spirkova, M., Stejskal, J., and Quadrat, O. 1999, Electrically Anisotropic Polyaniline-Polyurethane Composites, *Synthetic Metals*, Vol. 102, pp. 1264-1265.

- [8] Panigrahi, M.K., Majumdar, S.B., and Adhikari, B. 2011, H<sub>3</sub>PO<sub>4</sub>-doped DL-PLA/PANI composite for Methane gas sensing”, IEEE explorer, Vol. 97, pp. 1-7. ISBN: 978-1-4577-2035-2, 8-10 Dec. 2011, Nanoscience, Technology and Societal Implications (NSTSI), 2011 International Conference.2011, Vol. 97 (12), pp. 1-7.
- [9] Kumar, A., Jangir, L.K., Kumari, Y., Kumar, M., Kumar, V., and Awasthi, K., 2015, Optical and Structural Study of Polyaniline/Polystyrene Composite Films, Macromolecular symposia (Special Issue: Soft Materials,), Vol. 357, pp 229-234.
- [10] Gu, L., Zhao, X., Tong, X., Ma, J., Chen, B., Liu, S., Zhao, H., Yu, H., and Chen, J. 2016, Facile Preparation of Polyaniline Nanoparticles and Their Dispersion for Waterborne Anticorrosion Coatings, International Journal of Electrochemical Science, Vol. 11, pp. 1621-1631.
- [11] Shi, G., Rouabhia, M., Wang, Z., Dao, L.H., and Zhang, Z. 2004, A Novel Electrically Conductive and Biodegradable Composite Made of Polypyrrole Nanoparticles and Polylactide, Biomaterials, Vol. 25, pp. 2477-88.
- [12] Ruiz, J., Gonzalo, B., Dios, J.R., Laza, J.M., Vilas, J.L., and León, L.M. 2013, Improving the Processability of Conductive Polymers: The Case of Polyaniline, Advances in polymer Technology, Vol. 32, pp. 180-188.
- [13] Pozo-Gonzalo, C., Mecerreyes, D., Pomposo, J.A., Salsamendi, M., Marcilla, R., Grande, H., Vergaz, R., Barrios, D., and Sánchez-Pena, J.M., 2008, All-Plastic Electrochromic Devices based on PEDOT as Switchable Optical Attenuator in the Near IR, Solar Energy Materials: Solar Cells, Vol. 92, pp. 101-106.
- [14] Nguyen, T., Rendu, P. Le, Long, P., and Vos, S. De 2004, Chemical and Thermal Treatment of PEDOT: PSS Thin Films for Use in Organic Light Emitting Diodes, Surface Coating Technology, Vol. 180-181, pp. 646-649.
- [15] Hu, Z., Zhang, J., and Zhu, Y.2014, Effects of Solvent-Treated PEDOT:PSS on Organic Photovoltaic Devices, Renewable Energy, Vol. 62, pp. 100-105.
- [16] Bernards, D., Macaya, D., Nikolou, M., Defranco, J., Takamatsu, S., and Malliaras, G. 2008, Enzymatic Sensing with Organic Electrochemical Transistors, Journal of Materials Chemistry, Vol. 18, pp.116-120.
- [17] Li, J., Fang, K., Qiu, H., Li, S., and Mao, W. 2004, Micromorphology and Electrical Property of the HCl-Doped and DBSA-Doped Polyaniline, Synthetic Metals, Vol. 142, pp. 107-111.
- [18] Kapil, A., Taunk, M., and Chand, S. 2010, Preparation and Charge Transport Studies of Chemically Synthesized Polyaniline, Journal of Materials Science: Materials in Electronics, Vol. 21, pp. 399-404.

- [19] Bohli, N. Gmati, F., Mohamed, A.B., Vigneras, V., and Miane, J.-L. 2009, Conductivity Mechanism of Polyaniline Organic Films: The Effects of Solvent type and Casting Temperature, *Journal of Physics D Applied Physics*, Vol. 42, pp. 205404-xxx.
- [20] Long, Y.Z. Yin, Z.H., and Chen, Z.J. 2008, Low-Temperature Magnetoresistance Studies on Composite Films of Conducting Polymer and Multiwalled Carbon Nanotubes, *Journal of Physical Chemistry C*, Vol. 112, pp. 11507-11512.
- [21] Patil, A.O., Heeger, A.J., and Wudl, F. 1988, Optical Properties of Conducting Polymers, *Chemistry of Reviews*, Vol. 88, pp. 183-200.
- [22] Joshi, D.N., Atchuta, S.R., Reddy, L., Kumar, Y.N., and Sakthivel, A. 2019, Super-Hydrophilic Broadband Anti-reflective Coating with High Weather Stability for Solar and Optical Applications, *Solar Energy Materials and Solar Cells*, Vol. 200, pp. 110023-xxx.
- [23] Panigrahi, M.K. 2021, Investigation of Dc-Conductivity and Morphology of PMMA/PANI Composite, *International Research Journal of multidisciplinary Technovation*, Vol. 3, pp. 49-53.
- [24] Shobhana, E. 2012, X-Ray Diffraction and UV-Visible Studies of PMMA Thin Films, *International Journal of Modern Engineering Research (IJMER)*, Vol.2, pp-1092-1095.
- [25] Tomara, A.K., Mahendi, S., and Kumar, S. 2011, Structural Characterization of PMMA Blended with Chemically Synthesized PANi, *Advances in Applied Science Research*, Vol. 2, pp. 327-333.
- [26] Patricia L.B. Araujo, Katia A.S. Aquino, Elmo S. Araujo, (2007), Effects of Gamma Irradiation on PMMA/Polyaniline Nanofibre Composites, *Raman, International Journal of Low Radiation*, Vol. 4, pp. 149-160.
- [27] K.A. Ibrahim, (2017), Synthesis and Characterization of Polyaniline and Poly(aniline-co-o-Nitroaniline) using Vibrational Spectroscopy, *Arabian Journal of Chemistry*, Vol. 10, pp. 2668-2674.
- [28] Salma M. Hassan, (2013), Optical Properties of Prepared Polyaniline and Polymethylmethacrylate blends, *International Journal of Application or Innovation in Engineering & Management (IJAIEM)*, Vol. 2, pp. 19-22.
- [29] S. H. Deshmukh, D.K. Burghate, S.N. shilaskar, G.N. Chaudhan, P.T. Deshmikh, (2008), Optical Properties of Polyaniline Doped PVC-PMMA Thin Film, *Indian Journal of pure & applied physics*, Vol. 46, pp.344-348.
- [30] D. Farka, Andrew O.F. Jones, R. Menon, N. S. Sariciftci, P. Stadler, (2018), Metallic Conductivity Beyond the Mott Minimum in PEDOT: Sulphate at Low Temperatures, *Synthetic Metals*, Vol. 240, pp.59-66.
- [31] Timmer, B., Olthuis, W., and Van den Berg, A. Ammonia Sensors and Their

- Applications-A Review, 2005, Sensor and Actuators B: Chem., Vol. 107, pp. 666-677.
- [32] Dubbe, A. 2003, Fundamentals of Solid State Ionic Micro Gas Sensor, Sensor and Actuators B: Chemical, Vol. 88, pp. 138-148.
- [33] Mount, G.H., Rumburg, B., Havig, J., Lamb, B., Westberg, H., Yonge, D., Johnson, K., and Kincaid, R. 2002, Measurement of Atmospheric Ammonia at a Dairy using Differential Optical Absorption Spectroscopy in the Mid-Ultraviolet, Atmospheric Environment, Vol. 36, pp. 1799-1810.
- [34] Bidan, G. 1992, Electroconducting Conjugated Polymers: New Sensitive Matrices to Build up Chemical or Electrochemical Sensors – A Review, Sensor and Actuators B, Vol. 6, pp. 45-46.
- [35] de Lacy Costello, B.P.J., Evans, P., Guernion, N., Ratcliffe, N.M., Sivanand, P.S., and Teare, G.C. 2000, The Synthesis of a Number of 3-Alkyl and 3-Carboxy Substituted Pyrroles; Their Chemical Polymerisation onto Poly(Vinylidene Fluoride) Membranes, and Their Use as Gas Sensitive Resistors, Synthetic Metals, Vol. 114, pp. 181-188.
- [36] Riul Jr., A., Soto, A.M.G., Mello, S.V., Bone, S., Taylor, D.M., and Mattoso, L.H.C. 2003, An Electronic Tongue using Polypyrrole and Polyaniline, Synthetic Metals, Vol. 132, pp. 109-116.
- [37] Guernion, N., Ewen, R.J., Pihlainen, K., Ratcliffe, N.M., and Teare, G.C. 2002, The Fabrication and Characterization of a Highly Sensitive Polypyrrole Sensor and its Electrical Response to Amines of Differing Basicity at High Humidities, Synthetic Metals, Vol. 126, pp. 301-310.
- [38] Penza, M., Milella, E., Alba, M.B., Quirini, A., and Vasanelli, L. 1997, Selective NH<sub>3</sub> Gas Sensor based on Langmuir–Blodgett Polypyrrole Film, Sensor and Actuators B, Vol. 40, pp. 205-209.
- [39] Anitha, G., and Subramanian, E. 2003, Dopant Induced Specificity in Sensor Behaviour of Conducting Polyaniline Materials with Organic Solvents, Sensor and Actuators, Vol. 92, (2003) pp. 49-59.
- [40] Sakurai, Y., Jung, H.-S., Shimanouchi, T., Inoguchi, T., Morita, S., Kuboi, R., and Natsukuwa, K. 2002, Novel Array-Type Gas Sensors using Conducting polymers, and Their Performance for Gas Identification, Sensor and Actuators B, Vol. 83, pp. 270-275.
- [41] Lin, C.W., Hwang, B.J., and Lee, C.R. 1999, Sensing Behaviors of the Electrochemically Co-Deposited Polypyrrole-Poly(Vinylalcohol) Thin Film Exposed to Ammonia Gas, Materials Chemistry and Physics, Vol. 58, pp. 114-120.
- [42] Lee, Y.-S., Joo, B.-S., Choi, N.-J., Lim, J.-O., Huh, J.-S., and Lee, D.-D. 2003, Visible Optical Sensing of Ammonia based on Polyaniline Film,

Sensor and Actuators B, Vol. 93, pp. 148-152.

- [43] Rella, R., Siciliano, P., Quaranta, F., Primo, T., Valli, L., and Schenetti, L., 2002, Poly[3-(butylthio)thiophene] Langmuir–Blodgett Films as Selective Solid State Chemiresistors for Nitrogen Dioxide, *Colloids Surface A: Physicochemical Engineering Aspects*, Vol. 198, pp. 829-833.
- [44] Bai H., and Shi, G. 2007, Review Gas Sensors Based on Conducting Polymers, *Sensors*, Vol. 7, pp. 267-307.
- [45] Jin, Z., Su, Y.X., and Duan, Y.X. 2001, Development of a Polyaniline-based Optical Ammonia Sensor, *Sensor and Actuators B*, Vol. 72, pp. 75-79.
- [46] Nicho, M.E., Trejo, M., Garcia-Valenzuela, A., Saniger, J.M., Palacios, J., and Hu, H. 2001, Polyaniline Composite Coatings Interrogated by a Nulling Optical-Transmittance Bridge for Sensing Low Concentrations of Ammonia Gas, *Sensor and Actuators B*, Vol. 76, pp. 18-24.
- [47] Hu, H. Trejo, M., Nicho, M.E., Saniger, J.M., and Garcia-Valenzuela, A. 2002, Adsorption Kinetics of Optochemical NH<sub>3</sub> Gas Sensing with Semiconductor Polyaniline Films, *Sensor and Actuators B* Vol. 82, pp. 14-23.
- [48] Bekyarova, E., Davis, M., Burch, T., Itkis, M.E., Zhao, B., Sunshine, S., and Haddon, R.C. 2004, Chemically Functionalized Single-Walled Carbon Nanotubes as Ammonia Sensors, *Journal of Physical Chemistry B*, Vol. 108, pp. 19717-19720.
- [49] Hong, K.H., Oh, K.W., and Kang, T.J. 2004, Polyaniline-Nylon-6 Composite Fabric for Ammonia Gas Sensor, *Journal of Applied Polymer Science*, Vol. 92, pp. 37-42.
- [50] Liu, H.Q., Kameoka, J., Czaplewski, D.A., and Craighead, H.G. 2004, Polymeric Nanowire Chemical Sensor, *Nano Letter*, Vol. 4, pp. 671-675.
- [51] Honey Bourne, C.L., 1987, Solid Thin Films of Extended--Systems: Deposition, Characterization and Application, *Journal of Physics and Chemistry of Solids*, Vol. 48, pp. 109-141.
- [52] Liang, B., Yuan, C., and Wei, Y., 1997, Semiconducting, Gas Sensing Properties of Europium Bisphthalocyanine Langmuir–Blodgett Thin Films, *Journal of Vacuum Science & Technology B* Vol. 15, pp. 1432-1436.
- [53] Riul Jr., A., Mattoso, L.H.C., Melo, S.V., Telles, G.D., and Oliveria Jr., O.N., 1995, Langmuir and Langmuir–Blodgett Films of Parent Polyaniline Doped with Functionalized Acids, *Synthetic Metals*, Vol. 71, pp. 2067-2068.
- [54] Yadav, A., Agarwal, A., Agarwal, P.B., and Saini, P., 2015, Ammonia Sensing by PANI-DBSA Based Gas Sensor Exploiting Kelvin Probe Technique, *Journal of Nanoparticles* Vol. 2015, pp. 1-6.

- [55] Lv, D., Wenfeng D.L., Chen, S.W., Tan, R., Xu, L., and Song, W. 2021, PSS-PANI/PVDF Composite based Flexible nh Sensors with Sub-ppm Detection at Room Temperature, *Sensors and Actuators B: Chemical*, Vol. 328, pp. 129085-xxx.
- [56] Sutar, D.S., Padma, N., Aswal, D.K., Deshpande, S.K., Gupta, S.K., and Yakhmi, J.V., 2007, Preparation of Nanofibrous Polyaniline Films and Their Application as Ammonia Gas Sensor, *Sensors and Actuators B*, Vol. 128, pp. 286-292.
- [57] Crowley, K., Morrin, A., Hernandez, A., Malley, E.O., Whitten, P.G., Wallace, G.G., Smyth, M.R., and Killard, A.J. 2008, Fabrication of an Ammonia Gas Sensor using Inkjet-Printed Polyaniline Nanoparticles, *Talanta*, Vol. 77, pp. 710-717.
- [58] Matsuguchi, M., Io, J., Sugiyama, G., Sakai, Y. 2002, Effect of NH<sub>3</sub> Gas on the Electrical Conductivity of Polyaniline Blend Films, *Synthetic Metals*, Vol. 128, pp. 15-19.
- [59] Matsuguchi, M., Okamoto, A., Sakai, Y. 2003, Effect of Humidity on NH<sub>3</sub> Gas Sensitivity of Polyaniline Blend Films, *Sensors and Actuators B*, Vol. 94, pp. 46-52.
- [60] Deshpande, N.G., Gudage, Y.G., Sharma, R., Vyas, J.C., Kim, J.B., and Lee, Y.P. 2009, Studies on Tin Oxide-Intercalated Polyaniline Nanocomposite for Ammonia Gas Sensing Applications, *Sensors and Actuators B*, Vol. 138, pp. 76-84.
- [61] Tai, H., Jiang, Y., Xie, G., Yu, J., Chen, X., and Ying, Z. 2008, Influence of Polymerization Temperature on NH<sub>3</sub> Response of PANI/TiO<sub>2</sub> Thin Film Gas Sensor, *Sensors and Actuators B*, Vol. 129, pp. 319-326.